JOURNAL OF MATERIALS SCIENCE 21 (1986) 3038–3042

Latent hardening in polycrystalline copper and comparison with high density polyethylene

T. K. CHAKI, J. C. M. LI
Department of Mechanical Engineering, University of Rochester, Rochester, New York 14627, USA

When a parallelepiped specimen of polycrystalline copper is compressed in the x-direction (primary direction) while holding the z-dimension unchanged by a vice, the specimen is anisotropically hardened as follows: when the z-direction is subsequently compressed while holding the x-dimension unchanged the yield stress (0.2% offset) is higher than the final flow stress of the primary deformation. This is similar to latent hardening in single crystals. On the other hand, if the second compression is in the y-direction instead of the z-direction, the yielding (0.2% offset) occurs at a stress less than the final flow stress of the primary deformation. Both effects are reported here together with the results of two successive compressions in two mutually perpendicular directions without any constraints in either compression. These results are compared with the earlier results of high density polyethylene.

1. Introduction

The interaction between different slip systems is known as latent hardening in single crystals. This term is borrowed here to include the mutual effect of deformation in different directions. In view of the interaction between shear bands in polymers [1], the deformation in one direction should be affected by a prior deformation in another direction. Some preliminary experiments for polyethylene have been reported [2], including some early references on latent hardening in metals and ionic crystals.

Despite the severe interaction observed at the intersection of shear bands, the stress–strain curve for compression of a previously constrained direction whose dimension has been kept unchanged during a prior deformation in another direction is affected only slightly. A maximum effect [2] of 9% increase in flow stress was found for a 13% prior strain in another direction. This 9% was in comparison with the stress–strain curve without the prior deformation. This is a much smaller effect than the latent hardening in single crystals. There the flow stress in the latent system is even higher than the work hardened flow stress in the primary system.

The difference in behaviour between polymers and single crystals may be a result of an infinite variety of slip systems at least in the amorphous region of polymeric materials. These help pass through the shear bands developed during the primary deformation. If so, it seems that polycrystalline metals should behave like polymers and show limited interaction between deformations in different directions. A search of literature did not reveal the proper type of studies which yield such information. So a study is carried out for polycrystalline copper. Moreover, the results of latent hardening in polycrystalline copper will be useful to test new models [3] developed for polycrystals subjected to arbitrarily large strains.

Latent hardening in single crystals of copper was studied by Krisement, *et al.* [4]. The tensile direction for the primary deformation was $[\bar{1}\,2\,3]$ and the slip system was $(1\,1\,1)\,[\bar{1}\,0\,1]$. The second deformation was along $[\bar{3}\,2\,1]$ and the slip system was $(\bar{1}\,1\,\bar{1})\,[\bar{1}\,0\,1]$ which was the cross slip system of the primary. The critical resolved shear stress for the secondary deformation was 41% more than that of the work hardened resolved shear stress for the primary deformation between 7 and 16% primary shear strain. The second stage work hardening rate for the secondary deformtion was about 23% smaller than that for the primary deformation. Later studies were reported by Basinski and Jackson [5–8] and by Franciosi *et al.* [9]. The results were summarized by Michel and Champier [10] who used the following relation

$$\tau_l = A\tau_p + B \qquad (1)$$

where τ_p is the final resolved shear stress of the primary system, τ_l is the critical resolved shear stress of the latent system, and A and B are constants. For copper, data of Krisement *et al.* showed $A = 1.41$ and $B = 0$. Basinski and Jackson's data showed $A = 1.36$ and $B = 1.5$ MPa. Franciosi *et al.*'s [9] data at 200 K showed $A = 1.01$ and $B = 2.3$ MPa. These data will be compared with the present results on a polycrystalline copper.

2. Experimental details

Polycrystalline copper of Copper Development Association number 11 000, hot cast in cyclindrical form was obtained from Mueller Brass Company. The purity of copper was 99.9%. Rectangular pieces of copper were cut by a band saw and were then milled into rectangular shape of size 16.5 mm × 13.0 mm × 12.3 mm and polished to 1 μm by alumina slurries. The specimens were then annealed at 600° C for 2 h and furnace cooled. The average grain size after annealing was

0022–2461/86 $03.00 + .12

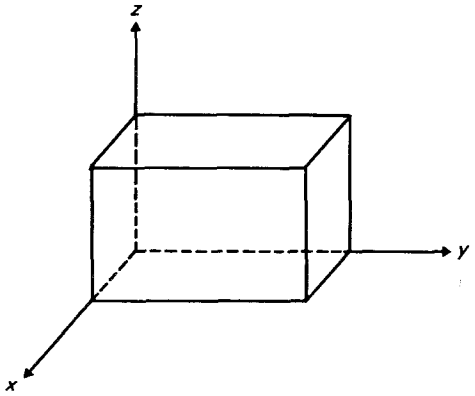

Figure 1 Schematic diagram showing the specimen geometry.

found by etching to be 40 μm. The material was isotropic as far as we could determine from grain shapes and from the stress–strain curves in different directions.

As shown in Fig. 1, the thickness direction (x-direction) was first compressed (primary deformation) while the width (z-direction) was constrained not to change by a vice (maximum change in the constrained dimension is less than 100 μm). The crosshead speed was 0.004 mm sec^{-1} corresponding to an initial strain rate of about 3.2 $\times$ 10^{-4} sec^{-1}. A hardened steel punch whose thickness was slightly smaller (by 50 μm) than the width of the specimen was used to compress the specimen by sliding between the jaws of the vice. A teflon film of 80 μm thick was covering all faces of the specimen for lubrication.

After the primary deformation, the specimen was taken out of the vice. Then the x-dimension was measured and compared with the original dimension to calculate the primary deformation. The specimen was then put back into the vice to constrain the new x-dimension (thickness which was just compressed) and at the same time to compress in the z-direction (width). This second compression was done by another punch whose size was slightly smaller than the new x-dimension so that it could slide between the jaws of the vice. The crosshead speed was again 0.004 mm sec^{-1} corresponding to an initial strain rate of about 3.1 $\times$ 10^{-4} sec^{-1}.

For another set of experiments the specimen was first compressed along the length (y-direction) while holding the width (z-direction) constrained. Then the thickness (x-direction) was compressed holding again the width (z-direction) constant. This second compression reversed the flow of the primary deformation. It is called the constrained softening experiment.

In a third set of experiments, both compressions were done on unconstrained specimens. The first compression was in the x-direction (thickness) and the second compression was in the z-direction (width). Since the primary or the first compression lengthened the other two dimensions, the second compression in either of the two other dimensions might be easier than the case without the primary deformation. Such softening will be called the unconstrained softening.

The load–displacement curves from the Instron chart were converted to true stress–true strain curves by determining the machine stiffness without the specimen and by assuming constant volume deformation. The true strain is the natural logarithm of the ratio of dimensions. The yield stress was calculated at 0.2% offset and at other offsets.

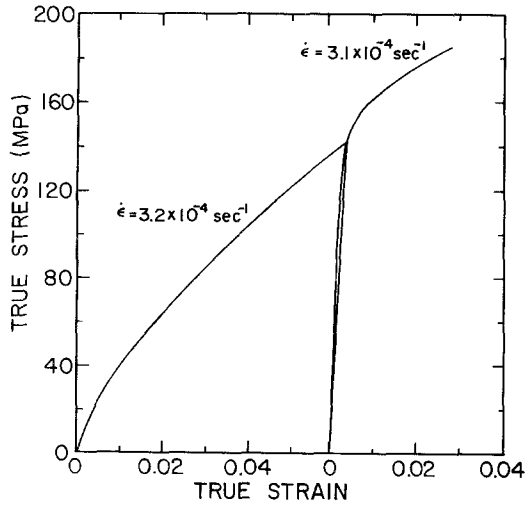

Figure 2 Stress–strain curves for the primary and the latent deformations.

3. Results

3.1. Latent hardening

The stress–strain curves for the primary deformation (x-direction) and for the subsequent latent deformation (z-direction) are shown in Fig. 2. The primary deformation was stopped at a final stress of 141.7 MPa. The unloading curve is a straight line with a slope of 3.90 $\times$ 10^4 MPa. The yielding (0.2% offset) during latent deformation occurs at a stress higher than the final primary stress. The latent hardening can be expressed by

$$\frac{\sigma_L}{\sigma_p} = \frac{\text{0.2\% offset yield stress during latent deformation}}{\text{final primary stress}} \quad (2)$$

In Fig. 2 the latent hardening is 1.06. The effect of primary strain (stress) on this ratio is shown in Fig. 3. It appears to have a maximum at about 5% primary strain.

Since the 0.2% offset is only a conventional way of estimating the yield stress without a yield point, other offsets were used also as shown in Fig. 3. Furthermore σ_L is plotted against σ_p in Fig. 4 in the light of Equation 1 as proposed by Michel and Champier [10]. It is seen that such relation is approximately obeyed with A = 1.0 and B ranging from 1 to 22 MPa depending on the offset. The A and B values are tabulated in Table I.

TABLE I Parameters for the linear relation of hardening and softening in different directions $\sigma = A\sigma_p + B$

Offset at which σ is calculated (%)	Latent hardening		Constrained softening		Unconstrained softening	
	A	B(MPa)	A	B(MPa)	A	B(MPa)
0.2	1.00	9.9	0.73	26.0	0.77	15.7
0.4	1.13	1.06	0.78	29.2	0.86	20.2
0.6	1.12	6.8	0.79	34.3	0.89	23.8
0.8	1.10	13.8	0.79	39.9	0.88	28.6
1.0	1.06	22.0	0.79	44.3	0.86	33.6

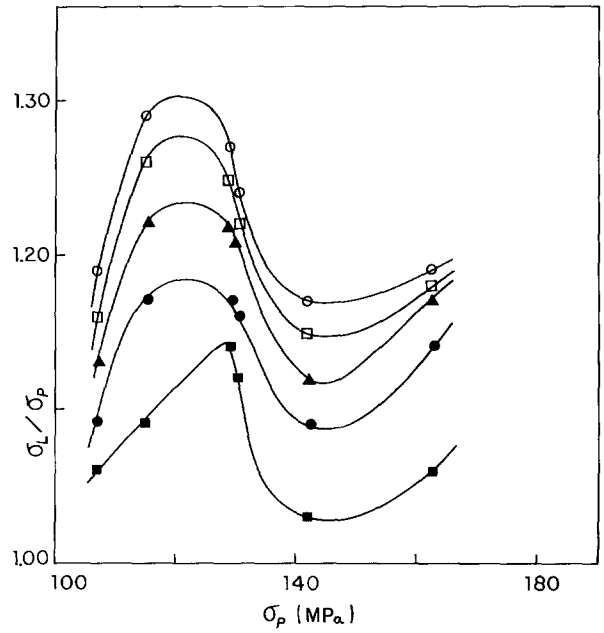

Figure 3 Latent hardening, (σ_L/σ_p) as a function of the final primary stress, σ_p for different offsets (%) used in calculating the latent yield stress. (○) 1.0%, (□) 0.8%, (▲) 0.6%, (●) 0.4%, (■) 0.2%.

3.2. Constrained softening or hardening

The stress–strain curve for the constrained softening experiment is shown in Fig. 5. The primary deformation along the length (y-direction) was stopped at a final stress of 162.0 MPa. The yielding (0.2% offset) during the secondary deformation along the x-direction occurs below the final primary stress. The amount of softening or hardening is expressed by

$$\frac{\sigma_c}{\sigma_p} = \frac{\text{0.2\% offset yield stress}}{\text{final primary stress}} \quad (3)$$

In Fig. 5 the softening is 5.4% since the 0.2% offset

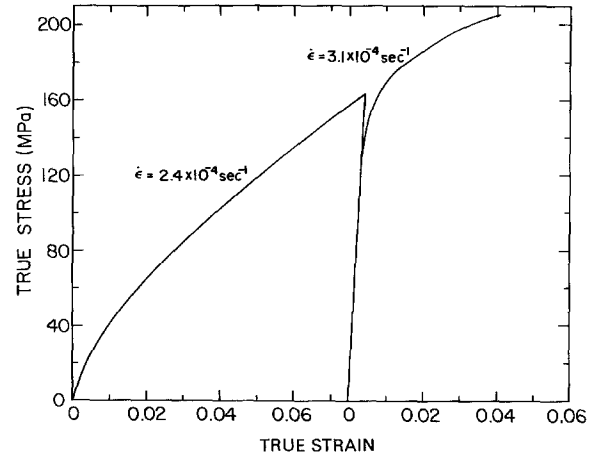

Figure 5 Stress–strain curves for the primary and the constrained deformations.

stress is below the final flow stress of the primary deformation. The work hardening rate in the secondary deformation is very high in the beginning. By the time the work hardening rate decreases to the same value as that of the primary deformation just before stopping, the flow stress is already higher than the final primary flow stress but about the same as the extrapolated flow stress to the same strain. Hence such consideration would indicate that there is really no softening in the secondary deformation.

As a function of primary strain, the constrained softening is shown in Fig. 6, for several offsets. Depending on the offset, the secondary deformation could be either softening or hardening. In general σ_c/σ_p is seen to decrease with increasing primary strain or stress.

According to Equation 1, σ_c is plotted against σ_p in Fig. 7 and it is seen that Equation 1 is approximately obeyed. The A and B values are tabulated in Table I.

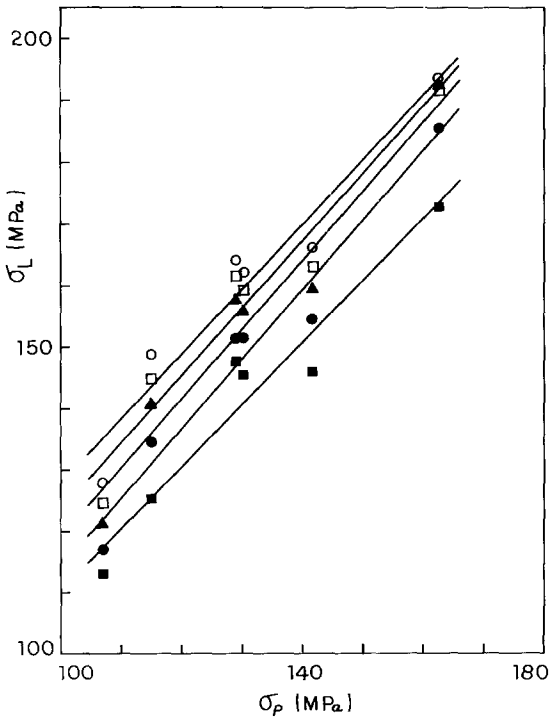

Figure 4 Latent yield stress, σ_L against the final primary stress, σ_p for different offsets (%). (○) 1.0%, (□) 0.8%, (▲) 0.6%, (●) 0.4%, (■) 0.2%.

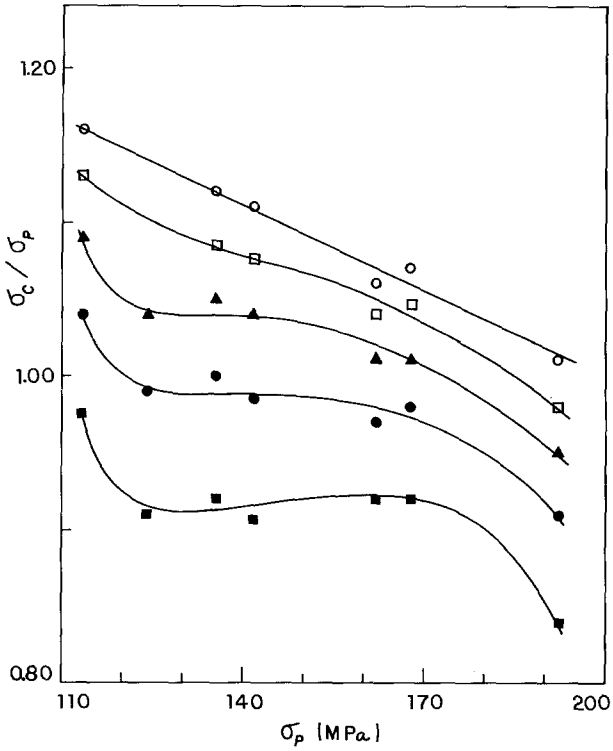

Figure 6 The ratio of the yield stress, σ_c, at different offsets (%) in the constrained soft direction and the final primary stress, σ_p, as a function of σ_p. (○) 1.0%, (□) 0.8%, (▲) 0.6%, (●) 0.4%, (■) 0.2%.

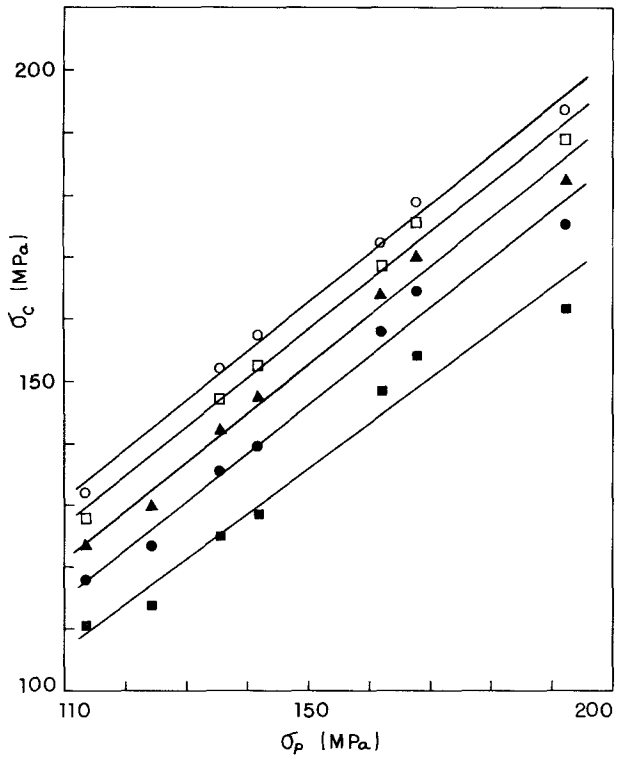

Figure 7 Yield stress, σ_c, at different offsets (%) in constrained soft direction against the final primary stress, σ_p. (○) 1.0%, (□) 0.8%, (▲) 0.6%, (●) 0.4%, (■) 0.2%.

3.3. Unconstrained softening or hardening

Fig. 8 shows the stress–strain curve during an unconstrained softening experiment. The primary deformation along the thickness (x-direction) was stopped at a final stress of 143.6 MPa. The softening defined by the 0.2% offset yield stress is 11.8%. The ratio σ_u/σ_p is plotted in Fig. 9 as a function of primary stress. Here again the ratio seems to decrease with increasing primary deformation.

In Fig. 10, σ_u is plotted against σ_p for several offsets. Equation 1 is again obeyed approximately. The A and B values are tabulated in Table I.

4. Discussion

4.1. Latent hardening

It is seen that latent hardening in polycrystalline copper is much larger than that in polyethylene. While in the former, the flow stress in the latent direction is higher than that of the primary direction, such is not the case in the latter. As mentioned earlier the stress–strain curve in the latent direction in polyethylene is only slightly higher than the case without primary deformation.

Such disparity in behaviour may be a good indication of different deformation mechanisms in polymers and

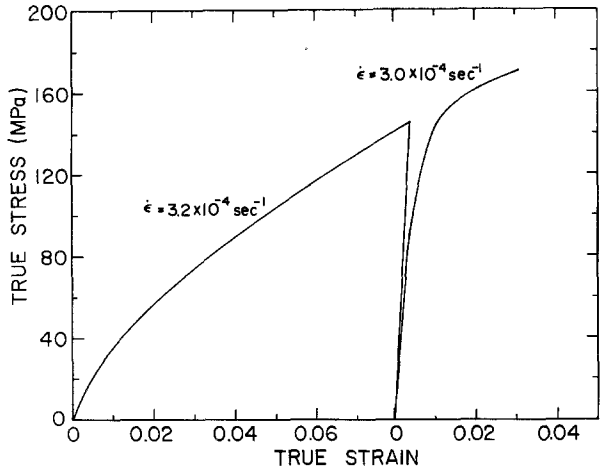

Figure 8 Stress–strain curves for the primary and unconstrained deformations.

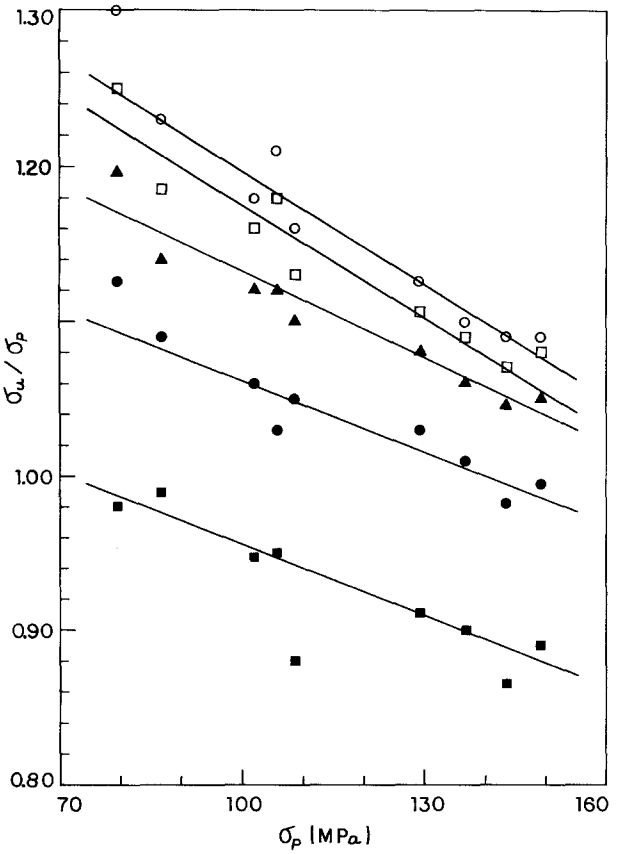

Figure 9 The ratio of the yield stress, σ_u, at different offsets (%) in the unconstrained soft direction and the final primary stress, σ_p as a function of σ_p. (○) 1.0%, (□) 0.8%, (▲) 0.6%, (●) 0.4%, (■) 0.2%.

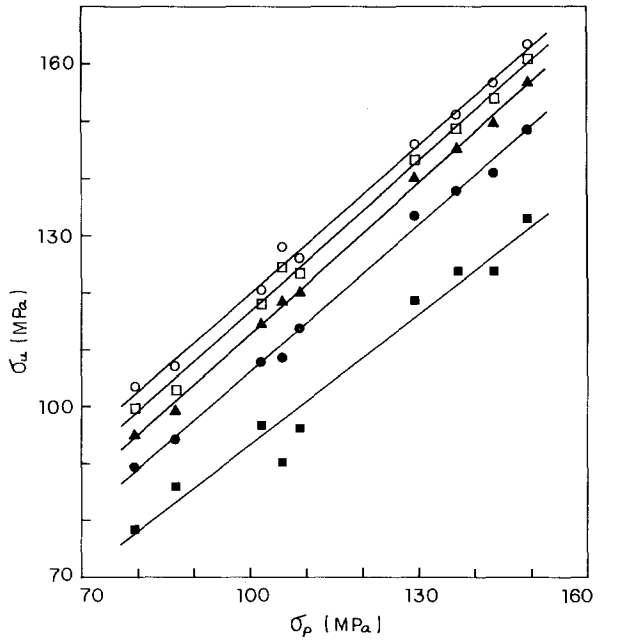

Figure 10 Yield stress, σ_u, at different offsets (%) in the unconstrained soft direction against the final primary stress, σ_p. (○) 1.0%, (□) 0.8%, (▲) 0.6%, (●) 0.4%, (■) 0.2%.

metals. In metals the motion of dislocations is the major cause of plastic deformation. The interaction between dislocations has a long range effect because of the large line tension of dislocations and a limited number of slip systems. For polymers in compression shear banding is the major cause of plastic deformation. Although there may be dislocations in shear bands, the interaction between these dislocations may have only local effects because of the small line tension of dislocations (no conservation of Burgers vector) and an infinite variety of slip systems.

While the interaction between shear bands in polymers may appear to be severe, the effect must be localized. As shown by a high speed movie study [11] the intersecting band still manages to propagate through an existing band at a reduction of speed by a factor of 3 only and resumes its normal speed as soon as it crosses the existing band. A dislocation, if it exists in a polymer, could dissociate into many dislocations of much smaller Burgers vectors so as to bypass obstacles at a stress of $\mu b/l$ (μ is the shear modulus, l is the spacing between obstacles) which can be made as small as possible by reducing b. While the net effect is the same after the intersection, namely, the local stresses could initiate cracks and shear bands, the external stress needed to overcome the intersection may not be too large.

For metals, the interaction between dislocations is so strong that $\mu b/l$ depends only on l since b is fixed. As shown in Fig. 2, the inital slope of the stress–strain curve in the latent direction is larger than the unloading slope of the primary deformation and is closer to Young's modulus of copper. This indicates a generally high stress for initiating dislocation motion in the microstrain region for the latent deformation than that for the primary deformation in its work hardened state. The initial work hardening rate for latent deformation is also high showing the tangling effect of existing dislocations produced by the primary deformation. However, because of the multiplicity of slip systems on polycrystals, the effect is not as large as the latent hardening in single crystals.

4.2. Constrained softening or hardening

The constrained softening is much larger in polymers than in metals. In polyethylene [2], the stress–strain curve in the constrained soft direction (Bauschinger softening) is lower than the case without the primary deformation. As shown in Fig. 5, the 0.2% offset yield stress in the constrained softening direction is only somewhat smaller than the work hardened flow stress of the primary deformation. It is still much larger than the case without the primary deformation. The rate of work hardening is also much higher than the undeformed material and by comparing at the same work hardening rate, there is no softening at all. In fact, the constrained softening becomes hardening at other offset yield stresses as shown in Fig. 6. All these can be attributed to the interaction between dislocations from different slip systems and the long range effect associated with such interactions. Without such strong interactions in polymers, the constrained softening can be understood fully by the Bauschinger effect since the flow is actually reversed.

4.3. Unconstrained softening or hardening

In polymers [2] the unconstrained softening is smaller than the constrained softening or Bauschinger softening. This is understandable because unconstrained softening should be about one-half of the constrained softening considering the amount of strain that is to be reversed. However, in metals the unconstrained softening is larger than the constrained softening. This can be attributed to the fact that for unconstrained deformation less slip systems are activated than constrained deformation. As a result the interaction between slip systems is less in the unconstrained deformation than in the constrained deformation. As in polymers the reduced interaction between slip systems helps the Bauschinger effect to make a discernible contribution to the softening. By taking larger offsets, the rapid work hardening wipes out completely the Bauschinger effect and the material shows unconstrained hardening instead.

Acknowledgements

We thank Dr Thomas Yu of Mueller Brass Co., Michigan for providing us with the pure copper sample. The work was supported by NSF through DMR-8211135 and by DOE through DE-FG02-85ER45201.

References

1. C. C. CHAU and J. C. M. LI, *J. Mater. Sci.* **14** (1979) 2172.
2. T. K. CHAKI and J. C. M. LI, *J. Appl. Phys.* **56** (1984) 2392.
3. R. J. ASARO and A. NEEDLEMAN, *Acta Metall.* **33** (1985) 923.
4. O. KRISEMENT, G. F. DE VRIES and F. BELL, *Phys. Status Solidi* **6** (1964) 73.
5. Z. S. BASINSKI and P. J. JACKSON, *Appl. Phys. Lett.* **6** (1965) 148.
6. *Idem, Phys. Status Solidi* **9** (1965) 805.
7. *Idem, ibid.* **10** (1965) 45.
8. P. J. JACKSON and Z. S. BASINSKI, *Can. J. Phys.* **45** (1967) 707.
9. P. FRANCIOSI, M. BERVEILLER and A. ZAOUI, *Acta Metall.* **28** (1980) 273.
10. J. P. MICHEL and G. CHAMPIER, *Single Cryst. Prop.* **B2** (1982) 21.
11. C. C. CHAU and J. C. M. LI, *J. Mater. Sci.* **17** (1982) 652.

Received 10 September
and accepted 11 October 1985